Contemporary Mathematics
https://ojs.wiserpub.com/index.php/CM/

Research Article

A Novel Hybrid Approach for Obtaining Approximate Series and Exact Solutions to the Caputo Fractional Black-Scholes Equations

Muhammad Imran Liaqat[1], Dumitru Baleanu[2], Majeed Ahmad Yousif[3], Thabet Abdeljawad[4,5,6], Pshtiwan Othman Mohammed[7,8,9*]

[1] Abdus Salam School of Mathematical Sciences, Government College University, 68-B, New Muslim Town, Lahore, 54600, Pakistan
[2] Department of Computer Science and Mathematics, Lebanese American University, Beirut, 11022801, Lebanon
[3] Department of Mathematics, College of Education, University of Zakho, Zakho, 42002, Iraq
[4] Department of Fundamental Sciences, Faculty of Engineering and Architecture, Istanbul Gelisim University, Avcılar-Istanbul, 34310, Turkiye
[5] Department of Mathematics and Sciences, Prince Sultan University, P.O. Box 66833, 11586, Riyadh, Saudi Arabia
[6] Department of Mathematics and Applied Mathematics, Sefako Makgatho Health Sciences University, Garankuwa, Medusa, 0204, South Africa
[7] Department of Mathematics, College of Education, University of Sulaimani, Sulaimani, 46001, Iraq
[8] Research Center, University of Halabja, Halabja, 46018, Iraq
[9] Research and Development Center, University of Sulaimani, Sulaymaniyah, 46001, Iraq
E-mail: pshtiwansangawi@gmail.com

Received: 16 June 2025; **Revised:** 19 August 2025; **Accepted:** 19 August 2025

Abstract: This study employs a novel approach to derive both approximate series and exact solutions to the fractional Black-Scholes model, utilizing the Elzaki transform and residual functions. This method is called the Elzaki Residual Method (ERM). By applying the basic limit principle at zero, the ERM demonstrates a superior ability to determine the coefficients of terms in the fractional power series, whereas other well-known methods such as the Adomian decomposition method, the variational iteration method, and the Homotopy perturbation method require integration, and the residual power series method relies on differentiation, both of which are challenging in fractional contexts. Moreover, the ERM outperforms series solution techniques that rely on Adomian and He's polynomials for solving nonlinear problems, as it eliminates the need for such polynomials. To verify the reliability of our approach, we perform recurrence and absolute error analyses. Additionally, comparative assessments with the projected method, the Adomian method, and the Aboodh decomposition method demonstrate strong agreement. Finally, graphical illustrations further confirm the accuracy of our solutions. Therefore, the ERM can serve as a valuable alternative for solving both linear and nonlinear fractional systems. Maple software is used to calculate the numerical and symbolic quantities in the paper.

***Keywords*:** Elzaki transform, Black-Scholes equations, Caputo derivative, residual functions

MSC: 35C07, 35C08, 35C09

DOI: https://doi.org/10.37256/cm.6520257484

1. Introduction

The fractional-order derivative is a generalization of the classical (integer-order) derivative to non-integer orders, allowing differentiation and integration of arbitrary real or complex orders. Unlike classical derivatives that depend solely on local behavior, fractional derivatives incorporate memory and hereditary properties of the system, as they are defined through integral operators that account for the entire history of a function. Common definitions include the Riemann-Liouville, Caputo, Hilfer, Hadamard, and Katugampola derivatives [1–5], each having specific advantages depending on the application and required initial conditions. These definitions are particularly useful for describing systems where the current state is influenced not only by instantaneous changes but also by accumulated past effects.

Fractional-order derivatives offer substantial advantages in mathematical modeling. They provide a more accurate and flexible framework for modeling real-world phenomena that exhibit memory, nonlocal interactions, or anomalous behavior-features that are difficult or impossible to capture with integer-order models. In engineering, physics, biology, and finance, fractional models have shown superior performance in simulating processes such as viscoelastic materials, diffusion in porous media, population dynamics, and electrical circuits with memory elements. Furthermore, The fractional order's tunability adds model flexibility, enabling better fitting to experimental data and more precise control in system design and analysis.

Among the various types of fractional-order derivatives, the Caputo fractional derivative stands as the most significant. It offers distinct advantages over alternative definitions, including the Riemann-Liouville, Grünwald-Letnikov, and Hadamard derivatives, particularly when solving initial value problems in Fractional Differential Equations (FDEs). These advantages include [6–9]:

1. **Physically Interpretable Initial Conditions:** The Caputo derivative allows the use of initial conditions in the same form as classical differential equations, i.e., using integer-order derivatives such as $\Im(0)$, $\Im'(0)$, etc. This is particularly useful in physical and engineering problems where initial values correspond to measurable quantities.

2. **Compatibility with Classical Models:** When the fractional order ν approaches an integer (e.g., $\nu \to 1$), the Caputo derivative naturally reduces to the classical derivative. This ensures a smooth transition from fractional to classical models.

3. **Ease of Numerical Implementation:** Many numerical methods, such as predictor-corrector algorithms and finite difference schemes, are more straightforward to implement using the Caputo derivative, especially for initial value problems.

4. **Wide Applicability in Real-World Problems:** Due to its clear interpretation of initial conditions, the Caputo derivative is widely used in modeling real-world systems with memory and hereditary properties in physics, biology, and engineering.

5. **Avoidance of Non-Physical Singularities:** Unlike the Riemann-Liouville derivative, the Caputo derivative avoids non-physical singularities at the initial point in many applications.

Mathematical modeling using FDEs has emerged as a powerful and versatile tool for representing complex dynamical systems more accurately than traditional integer-order models. Unlike classical differential equations that rely solely on local derivatives, fractional models incorporate nonlocal operators that account for the entire history of a system's evolution. This memory effect is particularly important when modeling phenomena where the future state depends not only on the current rate of change but also on past states. Fractional models can describe anomalous diffusion, viscoelasticity, non-exponential relaxation, and long-range temporal or spatial interactions, which cannot be adequately captured by integer-order models. The presence of fractional-order derivatives in the model allows for smoother transitions between states and finer control over system dynamics by adjusting the order of the derivative, making these models both flexible and physically meaningful.

Applications of FDEs span a wide range of scientific and engineering disciplines. In physics, FDEs are used to model anomalous diffusion and wave propagation in heterogeneous media. In engineering, they appear in control systems and signal processing, where memory effects are crucial for accurate system response. In biological and ecological systems, fractional models describe population dynamics, the spread of infectious diseases, and neuron firing processes, capturing the hereditary characteristics inherent in biological tissues. In economics and finance, they provide better models for

market memory and long-range dependence in financial time series. The ability of FDEs to accurately model real-world processes with memory and hereditary properties makes them a vital mathematical framework for developing predictive and reliable models across disciplines.

The solution of FDEs is essential because it provides critical insights into the behavior and dynamics of systems that exhibit memory, hereditary, and nonlocal properties-features commonly found in complex real-world phenomena. Unlike integer order models, which depend only on the current state of a system, fractional order models incorporate past states through fractional derivatives, making them more accurate and realistic. However, without solving these equations, either analytically or numerically, the advantages of such modeling remain purely theoretical. It is the solution that transforms the abstract mathematical formulation into meaningful, interpretable, and actionable insights about the physical, biological, or engineering system under study.

Moreover, solutions to FDEs are essential for prediction, control, and optimization. For instance, in viscoelastic materials, the stress depends not only on the present strain but also on the entire strain history-captured naturally by a fractional model. To design effective materials or processes, we must solve the FDE to predict stress responses. Similarly, in epidemiology, finance, and control theory, fractional models are used to describe spread, diffusion, or control mechanisms that are history dependent. Thus, finding the solution is not just a mathematical task; it is crucial for validating models, comparing them with experimental data, and applying them to solve real-world problems effectively.

In recent years, numerous techniques have been developed for solving FDEs, including Bernoulli sub-equation function method [10], sine-Gordon expansion method [11], the ansatz function scheme [12], Wang's direct mapping method [13], He's variational method [14], the semi-inverse approach [15], the Chebyshev polynomial technique [16], the Aboodh decomposition method [17], the operational matrix method [18], and the Shehu transform iterative technique [19]. For more details about the solution technique, see [20–22].

Integral transforms, among the most efficient techniques, are widely used to solve FDEs. Choosing an appropriate integral transform allows the conversion of a differential equation into a simpler algebraic equation. Recently, researchers have combined several powerful methods to develop alternative approaches for solving FDEs. Some of these combinations include the Elzaki Transform (ET) with residual functions [23]; the Shehu transform with the Adomian Decomposition Method (ADM) [24] and the natural transform with the homotopy perturbation method [25].

The Black-Scholes (BS) equation is one of the most influential mathematical formulations in financial market theory. It is a second-order parabolic partial differential equation that governs the pricing of financial derivatives. The BS framework for valuing stock options applies to a broad spectrum of assets and payoff structures.

The fractional BS model has gained significant attention in recent years due to its ability to incorporate memory and hereditary properties into financial modeling. This feature makes it more suitable for capturing the complex behavior of financial markets compared to the classical model. Key applications of the fractional BS model include [26]:

1. **Option Pricing with Market Memory:** The fractional BS model accounts for long-range dependence and memory effects in asset prices, providing more accurate pricing of financial derivatives such as European and American options.

2. **Volatility Modeling:** Real-world markets often exhibit time-varying and persistent volatility. Fractional calculus allows for better modeling of such behaviors, improving the reliability of volatility forecasting.

3. **Risk Management:** By incorporating memory effects, the model enhances the assessment of long-term risk and helps in developing more robust risk management strategies.

4. **Hedging Strategies:** Fractional models provide a more realistic framework for constructing hedging strategies, especially in markets with non-Markovian and fractal-like behavior.

5. **Interest Rate Modeling:** The model is also applied in the modeling of interest rates, particularly for capturing long-term dependencies and irregular fluctuations in yield curves.

6. **Pricing Exotic Options:** Exotic options, such as Asian, lookback, and barrier options, often depend on the path of the underlying asset. Fractional models are better suited for pricing these instruments due to their memory-sensitive characteristics.

7. **Financial Time Series Analysis:** The model is effective in analyzing and simulating financial time series data that exhibit anomalous diffusion, heavy tails, or self-similar behavior.

8. **Empirical Calibration:** Fractional models can be calibrated to historical market data more accurately than classical models, making them valuable tools for empirical finance and quantitative analysis.

The value of an option under the BS model is described by the following equation:

$$\frac{\partial^{\nu}\Im(\mathrm{x},\,\tau)}{\partial\tau^{\nu}}+\frac{\eta^2\mathrm{x}^2}{2}\frac{\partial^2\Im(\mathrm{x},\,\tau)}{\partial\mathrm{x}^2}+\mathrm{U}(\tau)\mathrm{x}\frac{\partial\Im(\mathrm{x},\,\tau)}{\partial\mathrm{x}}-\mathrm{U}(\tau)\Im(\mathrm{x},\,\tau)=0,\ (\mathrm{x},\,\tau)\in\mathrm{R}^{+}\times(0,\,\mathrm{A}),\tag{1}$$

$\Im(\mathrm{x},\,\tau)$ represent the valuation of a European option at the underlying asset price x and time τ. The volatility of the company's stock, denoted by η, characterizes the dispersion or variability in the asset's returns. The symbol A denotes the maturity date of the option, while $\mathrm{U}(\tau)$ refers to the risk-free interest rate prevailing at time τ. The notations $\Im_c(\mathrm{x},\tau)$ and $\Im_p(\mathrm{x},\,\tau)$ respectively denote the European call and put option prices. The corresponding payoff functions are expressed as $\Im_c(\mathrm{x},\,\tau)=\max(\mathrm{x}-\mathrm{Z},\,0)$ and $\Im_p(\mathrm{x},\,\tau)=\max(\mathrm{Z}-\mathrm{x},\,0)$, where Z is the strike price (or exercise price) of the option. The function $\max(\mathrm{x},\,0)$ returns the greater of x and zero, capturing the non-negative nature of option payoffs. The crucial aspect of the BS equation from a financial perspective is that it reduces risk by enabling judicious buying and selling of the under-reviewed stock. This demonstrates that the BS model yields a unique option price. The crucial aspect of the BS equation from a financial perspective is that it reduces risk by enabling judicious buying and selling of the under-reviewed stock. This article presents a fractional model for pricing various financial derivatives.

Finding solutions to time-fractional BS models is an interesting and important topic for researchers. Kadalbajoo et al. [27] used the uniform cubic B-spline collocation method to find the numerical solution of the BS model. Edeki et al. [28] used a newly developed semi-analytic method known as the projected differential transform method to arrive at analytical solutions to the time-fractional BS model for the European call option. This algorithmic approach is an adaptation of the traditional differential transformation methodology. Using an iterative process, Yavuz and Ozdemir [29] obtained the approximate solution of the fractional BS models. The conformable derivative is the fractional differentiation operator utilized in this study. The fractional BS equation was solved by Alfaqeih and Ozis [30] using the Aboodh transform decomposition technique. This technique combines the Adomian decomposition method and the Aboodh transform. Saratha et al. [31] analyzed the time-fractional BS models using the homotopy analysis approach. In the context of Caputo, the fractional derivative is taken into consideration. Edeki et al. [32] used a coupled method known as the fractional complex transform with a modified differential transform method to offer analytical solutions for the fractional BS models. For more details about the solutions to BS models, see [33–37].

This study employs the coupled ET and residual functions approach, in the Caputo Derivative (CD) sense, to solve time-fractional BS models. The reliability of the method is demonstrated through both numerical and graphical analyses. Tables 1-3 present the recurrence errors obtained from the fifth-step approximation for various values of ν, illustrating that the errors decrease as $\nu\to 1.0$. A comparative analysis of absolute errors between the ERM, the Projected Differential Transform Approach (PDTA) [28], the ADM [29], and Aboodh ADM [30] is presented in Tables 4-6. The results show complete consistency between ERM and the reference methods, including PDTA, ADM, and Aboodh ADM. Consequently, the ERM can effectively replace existing methods such as the Residual Series Approach and techniques based on He's or Adomian polynomials for solving FDEs. Moreover, this method eliminates the need for restrictive assumptions about the system's physical properties, thereby addressing a major limitation of conventional perturbation-based approaches.

The structure of this research work is as follows: The next Section 2 presents definitions and key results from the theory of fractional calculus. In Section 3, the core concept of the ERM is explored to derive analytical solutions for the time-fractional BS models. Section 4 demonstrates the reliability and simplicity of the proposed method through three illustrative problems. In Section 5, the results obtained using ERM are analyzed using graphs and tables. Finally, the conclusion is presented in Section 6.

2. Preliminaries

This section presents important preliminaries that form the foundation of the findings in this research study.

Definition 1 [38] If the function $\Im(x,\ \tau)$ meets the existence conditions for the ET, its ET is expressed as:

$$E[\Im(x,\ \tau)] = \aleph(x,\ \omega) = \omega \int_0^{\infty} \Im(x,\ \tau) e^{-\frac{\tau}{\omega}} d\tau,\ \tau \geq 0,\ e_1 \leq \omega \leq e_2. \tag{2}$$

Lemma 1 [39] Suppose that the existence conditions of the ET are fulfilled by the functions $\Im_1(x,\ \tau)$ and $\Im_2(x,\ \tau)$. Consequently, we have $E[\Im_1(x,\ \tau)] = \aleph_1(x,\ \omega)$ and $E[\Im_2(x,\ \tau)] = \aleph_2(x,\ \omega)$, where ρ_1 and ρ_2 are constants. Under these assumptions, the following properties hold:

(i) $E[\rho_1\Im_1(x,\ \tau) + \rho_2\Im_2(x,\ \tau)] = \rho_1\aleph_1(x,\ \omega) + \rho_2\aleph_2(x,\ \omega)$,

(ii) $E^{-1}[\rho_1\aleph_1(x,\ \omega) + \rho_2\aleph_2(x,\ \omega)] = \rho_1\Im_1(x,\ \tau) + \rho_2\Im_2(x,\ \tau)$,

(iii) $\Theta_0(x) = \lim_{\omega\to 0}\left(\frac{1}{\omega^2}\aleph(x,\ \omega)\right) = \Im(x,\ 0)$.

(iv) $E[D_\tau^\nu \Im(x,\ \tau)] = \frac{1}{\omega^\nu}\aleph(x,\ \omega) - \sum_{i=0}^{n-1}\frac{\Im^{(i)}(x,\ 0)}{\omega^{\nu-i-2}},\ n-1 < \nu \leq n,\ n \in \mathbb{N}$.

(v) $E[D_\tau^{n\nu} \Im(x,\ \tau)] = \frac{1}{\omega^{n\nu}}\aleph(x,\ \omega) - \sum_{i=0}^{n-1}\omega^{\nu(i-n)+2} D_\tau^{i\nu}\Im(x,\ 0),\ 0 < \nu \leq 1$.

Definition 2 [39] The fractional derivatives of $\Im(x,\ \tau)$ of order ν in the CD sense is defined as follows:

$$D_\tau^\nu \Im(x,\ \tau) = \Im_\nu^{r-\nu}\Im^{(n)}(x,\ \tau),\ \tau \geq 0,\ n-1 < \nu \leq n, \tag{3}$$

where $\Im_\tau^{n-\nu}$ is the Riemann-Liouville (R-L) integral of $\Im(x,\ \tau)$.

Theorem 1 [39] Consider that the expression $E[\Im(x,\ \tau)] = \aleph(x,\ s)$ can be expressed through a Multiple Fractional Power Series (MFPS) formulation.

$$\aleph(x,\ \omega) = \sum_{n=0}^{\infty} \Theta_n(x)\omega^{n\nu+2}, \tag{4}$$

then we have

$$\Theta_n(x) = D_\tau^{n\nu}\Im(x,\ 0), \tag{5}$$

where, $D_\tau^{n\nu} = D_\tau^\nu . D_\tau^\nu \ldots D_\tau^\nu (n - times)$.

3. The algorithm of ERM

The following stages can be used to summarize the core algorithm of this approach to solving BS models: The ET is used to solve the problem. As a result, the problem has an algebraic structure in the ET space. The solution to the algebraic equation generated in the first stage is presented in the second step utilizing the new MFPS. Limit concepts are used to establish the coefficients of the MFPS. Therefore, by considering the inverse ET, we have identified a solution to the problem in the original space.

Step 1: Equation (1) can be reformulated as follows:

$$D_\tau^\nu \Im(x,\ \tau) - g\left(\Im(x,\ \tau),\ \frac{\eta^2 x^2 \partial^2 \Im(x,\ \tau)}{2\partial x^2},\ U(\tau)x\frac{\partial \Im(x,\ \tau)}{\partial x},\ U(\tau)\Im(x,\ \tau)\right) = 0. \tag{6}$$

Step 2: Applying the ET to both sides of Eq. (6) yields:

$$\aleph(\mathrm{x},\ \omega) - \omega^2 \Im(\mathrm{x},\ 0) - \omega^{\nu} G(\mathrm{x},\ \omega) = 0, \tag{7}$$

where

$$\mathrm{E}[\Im(\mathrm{x},\ \tau)] = \aleph(\mathrm{x},\ \omega),$$

and

$$G(\mathrm{x},\ \omega) = \mathrm{E}\left[g\left(\frac{\eta^2 \mathrm{x}^2 \partial^2 \Im(\mathrm{x},\ \tau)}{2\partial \mathrm{x}^2},\ \mathrm{U}(\tau)\Im(\mathrm{x},\ \tau),\ \Im(\mathrm{x},\ \tau),\ \mathrm{U}(\tau)\mathrm{x}\frac{\partial \Im(\mathrm{x},\ \tau)}{\partial \mathrm{x}} \right) \right].$$

Step 3: Suppose the solution to Eq. (7) takes the following series form:

$$\aleph(\mathrm{x},\ \omega) = \sum_{\mathrm{n}=0}^{\infty} \Theta_{\mathrm{n}}(\mathrm{x}) \omega^{\mathrm{n}\mathrm{x}+2}. \tag{8}$$

Step 4: From Lemma 1 (iii), we deduce:

$$\Theta_0(\mathrm{x}) = \lim_{\omega \to 0} \left(\frac{1}{\omega^2} \aleph(\mathrm{x},\ \omega) \right) = \Im(\mathrm{x},\ 0). \tag{9}$$

Step 5: Let the $\Bbbk$th-order truncated form of $\aleph(\mathrm{x},\ \omega)$ be defined as:

$$\aleph_{\Bbbk}(\mathrm{x},\ \omega) = \Theta_0(\mathrm{x})\omega^2 + \sum_{\mathrm{n}=1}^{\Bbbk} \Theta_{\mathrm{n}}(\mathrm{x}) \omega^{\mathrm{n}\nu+2}. \tag{10}$$

Step 6: The Elzaki Residual Function (ERF) of Eq. (7), and its $\Bbbk$th-order ERF are given respectively by:

$$\mathrm{ERes}(\mathrm{x},\ \omega) = \aleph(\mathrm{x},\ \omega) - \omega^2 \Theta_0(\mathrm{x}) - \omega^{\nu} G(\mathrm{x},\ \omega), \tag{11}$$

$$\mathrm{ERes}_{\Bbbk}(\mathrm{x},\ \omega) = \aleph_{\Bbbk}(\mathrm{x},\ \omega) - \omega^2 \Theta_0(\mathrm{x}) - \omega^{\nu} G_{\Bbbk}(\mathrm{x},\ \omega). \tag{12}$$

Step 7: Substitute the truncated expansion $\aleph_{\Bbbk}(\mathrm{x},\ \omega)$ into the residual expression $\mathrm{ERes}_{\Bbbk}(\mathrm{x},\ \omega)$.
Step 8: Multiply both sides of $\mathrm{ERes}_{\Bbbk}(\mathrm{x},\ \omega)$ by $\omega^{\Bbbk\nu+2}$.
Step 9: Using Eq. (12), determine each coefficient $\Theta_{\mathrm{n}}(\mathrm{x})$ for $\mathrm{n} = 1,\ 2,\ 3,\ \ldots,\ \Bbbk$ sequentially by solving:

$$\lim_{\omega\to 0}\left(\frac{1}{\omega^{\mathbb{k}\nu+2}}\mathrm{ERes}_{\mathbb{k}}(\mathrm{x},\ \omega)\right)=0,\quad \mathbb{k}=1,\ 2,\ 3,\ \ldots \tag{13}$$

Step 10: Applying the acquired values of $\Theta_{\mathrm{n}}(\mathrm{x})$ to the $\mathbb{k}$th-order truncated form of $\aleph(\mathrm{x},\ \omega)$ for all $\mathrm{n}=1$ to $\mathbb{k}$ results in the $\mathbb{k}$th-order approximate solution of Eq. (7).

Step 11: Upon operating E^{-1} on the conclusive expression of $\aleph_{\mathbb{k}}(\mathrm{x},\ \omega)$, we derive the $\mathbb{k}$th-order approximate solution $\Im_{\mathbb{k}}(\mathrm{x},\ \tau)$ to the presented problem.

The subsequent theorem provides a detailed explanation and establishes the convergence criteria for the revised version of Fractional Power Series (FPS).

Theorem 2 Let $\mathrm{E}_{\nu}[\Im(\mathrm{x},\ \tau)]=\aleph(\mathrm{x},\ \omega)$ be represented as the novel form of FPS $\aleph(\mathrm{x},\ \omega)=\sum_{\mathrm{n}=0}^{\infty}\omega^{\mathrm{n}\nu+2}\aleph_{\mathrm{n}}(\mathrm{x})$. If the following condition is fulfilled

$$\left|\frac{1}{\omega^{2}}\mathrm{E}_{\nu}[\mathrm{D}_{\tau}^{(\mathrm{n}+1)}\Im(\mathrm{x},\ \tau)\right|\leq \mathrm{Z},$$

then $\mathbb{R}_{\mathrm{n}}(\mathrm{x},\ \omega)$ of the novel form of FPS fulfills the following:

$$\left|\mathbb{R}_{\mathrm{n}}(\mathrm{x},\ \omega)\right|\leq \omega^{(\mathrm{n}+1)\nu+2}\mathrm{Z}.$$

Proof. Take into consideration the following from the FPS:

$$\mathbb{R}_{\mathrm{n}}(\mathrm{x},\ \omega)=\Im(\mathrm{x},\ \omega)-\sum_{\kappa=0}^{\mathrm{n}}\omega^{\kappa\nu+2}\aleph_{\kappa}(\mathrm{x}). \tag{14}$$

Eq. (14) converts through the application of Theorem 1 as follows:

$$\mathbb{R}_{\mathrm{n}}(\mathrm{x},\ \omega)=\Im(\mathrm{x},\ \omega)-\sum_{\kappa=0}^{\mathrm{n}}\omega^{\kappa\nu+2}\mathrm{D}_{\tau}^{\kappa\nu}\Im(\mathrm{x},\ 0). \tag{15}$$

Divide both sides of Eq. (15) by $\omega^{(\mathrm{n}+1)\nu+2}$. As a result, we have the following:

$$\frac{1}{\omega^{(\mathrm{n}+1)\nu+2}}\mathbb{R}_{\mathrm{n}}(\mathrm{x},\ \omega)=\frac{1}{\omega^{2}}\left(\frac{1}{\omega^{(\mathrm{n}+1)\nu}}\Im(\mathrm{x},\ \omega)-\sum_{\kappa=0}^{\mathrm{n}}\frac{1}{\omega^{(\mathrm{n}+1-\kappa)\nu-2}}\mathrm{D}_{\tau}^{\kappa\nu}\Im(\mathrm{x},\ 0)\right). \tag{16}$$

When Lemma 1 (v) is applied to Eq. (16), we obtain:

$$\frac{1}{\omega^{(\mathrm{n}+1)\nu+2}}\mathbb{R}_{\mathrm{n}}(\mathrm{x},\ \omega)=\frac{1}{\omega^{2}}\mathrm{E}\left[\mathrm{D}_{\tau}^{(\mathrm{n}+1)\nu}\Im(\mathrm{x},\ \tau)\right]. \tag{17}$$

By utilizing the absolute value notation in Eq. (17), we obtain:

$$\left|\frac{1}{\omega^{(n+1)\nu+2}}\mathbb{R}_n(x,\ \omega)\right| = \left|\frac{1}{\omega^2}E\left[D_\tau^{(n+1)\nu}\Im(x,\ \tau)\right]\right|. \tag{18}$$

A specific result is obtained by applying the provided condition to Eq. (18).

$$\left|\frac{1}{\omega^{(n+1)\nu+2}}\mathbb{R}_n(x,\ \omega)\right| \leq Z.$$

$$-Z\omega^{(n+1)\nu+2} \leq \mathbb{R}_n(x,\ \omega) \leq Z\omega^{(n+1)\nu+2}. \tag{19}$$

The required result is obtained from Eq. (19).

$$\left|\mathbb{R}_n(x,\ \omega)\right| \leq Z\omega^{(n+1)\nu+2}.$$

4. Applications

This section presents three time-fractional BS models to demonstrate the efficiency of the ERM.
Problem 4.1 The first BS model is given below [32]:

$$\frac{\partial^\nu \Im(x,\ \tau)}{\partial \tau^\nu} + x^2\frac{\partial^2\Im(x,\ \tau)}{\partial x^2} + 0.5x\frac{\partial\Im(x,\ \tau)}{\partial x} - \Im(x,\ \tau) = 0, \quad 0 < \nu \leq 1, \tag{20}$$

with

$$\Im(x,\ 0) = \max(x^3,\ 0) = \begin{cases} x^3 & \text{for } x > 0, \\ \\ 0 & \text{for } x \leq 0. \end{cases} \tag{21}$$

Here we will discuss case $x > 0$.
E is used on both sides of Eq. (20).

$$E\left[\frac{\partial^\nu \Im(x,\ \tau)}{\partial \tau^\nu} + x^2\frac{\partial^2\Im(x,\ \tau)}{\partial x^2} + 0.5x\frac{\partial\Im(x,\ \tau)}{\partial x} - \Im(x,\ \tau)\right] = 0. \tag{22}$$

By utilizing the procedure described in Section 3, the following result is drawn from Eq. (22):

$$\aleph(x,\ \omega) = x^3\omega^2 - \omega^\nu x^2 D_{xx}E[\Im(x,\ \tau)] - 0.5\omega^\nu x D_x E[\Im(x,\ \tau)] + \omega^\nu E[\Im(x,\ \tau)]. \tag{23}$$

We assume that $\aleph(x,\ \omega)$ expands to the following:

$$\aleph(\mathrm{x},\ \omega) = \sum_{\mathrm{n}=0}^{\infty} \Theta_{\mathrm{n}}(\mathrm{x})\omega^{\mathrm{n}\nu+2}. \tag{24}$$

The following is the $\Bbbk$th-truncated series:

$$\aleph_{\Bbbk}(\mathrm{x},\ \omega) = \sum_{\mathrm{n}=0}^{\infty} \Theta_{\mathrm{n}}(\mathrm{x})\omega^{\mathrm{n}\nu+2}. \tag{25}$$

By utilizing Lemma 1 (iii), we get the following result:

$$\Theta_0(\mathrm{x}) = \lim_{\omega\to 0}\left(\frac{1}{\omega^2}\aleph(\mathrm{x},\ \omega)\right) = \Im(\mathrm{x},\ 0) = \mathrm{x}^3.$$

As a result, the $\Bbbk$th-truncated expansion is as follows:

$$\aleph_{\Bbbk}(\mathrm{x},\ \omega) = \mathrm{x}^3\omega^2 + \sum_{\mathrm{n}=1}^{\Bbbk} \Theta_{\mathrm{n}}(\mathrm{x})\omega^{\mathrm{n}\nu+2}. \tag{26}$$

The ERF and $\Bbbk$th-ERF of Eq. (23) are given below:

$$\mathrm{E}Res(\mathrm{x},\ \omega) = \aleph(\mathrm{x},\ \omega) - \mathrm{x}^3\omega^2 + \omega^{\nu}\mathrm{x}^2\mathrm{D}_{\mathrm{xx}}\aleph(\mathrm{x},\ \omega) + \frac{1}{2}\omega^{\nu}\mathrm{x}\mathrm{D}_{\mathrm{x}}\aleph(\mathrm{x},\ \omega) - \omega^{\nu}\aleph(\mathrm{x},\ \omega). \tag{27}$$

$$\mathrm{E}Res_{\Bbbk}(\mathrm{x},\ \omega) = \aleph_{\Bbbk}(\mathrm{x},\ \omega) - \mathrm{x}^3\omega^2 + \omega^{\nu}\mathrm{x}^2\mathrm{D}_{\mathrm{xx}}\aleph_{\Bbbk}(\mathrm{x},\ \omega) + \frac{1}{2}\omega^{\nu}\mathrm{x}\mathrm{D}_{\mathrm{x}}\aleph_{\Bbbk}(\mathrm{x},\ \omega) - \omega^{\nu}\aleph_{\Bbbk}(\mathrm{x},\ \omega). \tag{28}$$

We expand the residual series approach attributes to emphasize the following specifics:
(i) $\mathrm{E}Res(\mathrm{x},\ \omega) = 0$ and $\lim_{\Bbbk\to\infty} \mathrm{E}[Res_{\Bbbk}(\mathrm{x},\ \omega)]$,
(ii) $\lim_{\omega\to 0}\left(\frac{1}{\omega^2}\mathrm{E}Res(\mathrm{x},\ \omega)\right) = 0 \implies \lim_{\omega\to 0}\left(\frac{1}{\omega^2}\mathrm{E}Res_{\Bbbk}(\mathrm{x},\ \omega)\right) = 0$,
(iii) $\lim_{\omega\to 0}\left(\frac{1}{\omega^{\Bbbk\nu+2}}\mathrm{E}Res(\mathrm{x},\ \omega)\right) = \lim_{\omega\to 0}\left(\frac{1}{\omega^{\Bbbk\nu+2}}\mathrm{E}Res_{\Bbbk}(\mathrm{x},\ \omega)\right) = 0, \Bbbk = 1,\ 2,\ 3, \ldots.$
To find the $\Theta_1(\mathrm{x})$, first plug the $\aleph_1(\mathrm{x},\ \omega) = \mathrm{x}^3\omega^2 + \Theta_1(\mathrm{x})\omega^{\nu+2}$ into the $\mathrm{E}Res_1(\mathrm{x},\ \omega)$.

$$\mathrm{E}Res_1(\mathrm{x},\ \omega) = \left[\mathrm{x}^3\omega^2 + \Theta_1(\mathrm{x})\omega^{\nu+2}\right] - \mathrm{x}^3\omega^2 + \omega^{\nu}\mathrm{x}^2\mathrm{D}_{\mathrm{xx}}\left[\mathrm{x}^3\omega^2 + \Theta_1(\mathrm{x})\omega^{\nu+2}\right]$$

$$+ \frac{1}{2}\omega^{\nu}\mathrm{x}\mathrm{D}_{\mathrm{x}}\left[\mathrm{x}^3\omega^2 + \Theta_1(\mathrm{x})\omega^{\nu+2}\right] - \omega^{\nu}\left[\mathrm{x}^3\omega^2 + \Theta_1(\mathrm{x})\omega^{\nu+2}\right]. \tag{29}$$

By dividing $\omega^{\nu+2}$ on both sides of Eq. (29), we get

$$\frac{1}{\omega^{\nu+2}}\mathrm{E}Res_1(\mathrm{x},\ \omega)=\Theta_1(\mathrm{x})+\mathrm{x}^2\mathrm{D}_{\mathrm{xx}}\left[\mathrm{x}^3+\Theta_1(\mathrm{x})\omega^{\nu}\right]+\frac{1}{2}\mathrm{x}\mathrm{D}_{\mathrm{x}}\left[\mathrm{x}^3+\Theta_1(\mathrm{x})\omega^{\nu}\right]-\left[\mathrm{x}^3+\Theta_1(\mathrm{x})\omega^{\nu}\right]. \tag{30}$$

Using the following formula,

$$\lim_{\omega\to 0}\left(\frac{1}{\omega^{\Bbbk\nu+2}}\mathrm{E}Res_{\Bbbk}(\mathrm{x},\ \omega)\right)=0,\ \text{when}\ \Bbbk=1. \tag{31}$$

As a consequence, we got the following results:

$$\Theta_1(\mathrm{x})=-6.5\mathrm{x}^3.$$

Similarly, to find $\Theta_2(\mathrm{x})$, we have to use the $\aleph_2(\mathrm{x},\ \omega)=\mathrm{x}^3\omega^2+\Theta_1(\mathrm{x})\omega^{\nu+2}+\Theta_2(\mathrm{x})\omega^{2\nu+2}$ into the $2nd$-ERF.

$$\begin{aligned}\mathrm{E}Res_2(\mathrm{x},s)=&\left[\mathrm{x}^3\omega^2+\Theta_1(\mathrm{x})\omega^{\nu+2}+\Theta_2(\mathrm{x})\omega^{2\nu+2}\right]-\mathrm{x}^3\omega^2+\omega^{\nu}\mathrm{x}^2\mathrm{D}_{\mathrm{xx}}\left[\mathrm{x}^3\omega^2+\Theta_1(\mathrm{x})\omega^{\nu+2}+\Theta_2(\mathrm{x})\omega^{2\nu+2}\right]\\&+\frac{1}{2}\omega^{\nu}\mathrm{x}\mathrm{D}_{\mathrm{x}}\left[\mathrm{x}^3\omega^2+\Theta_1(\mathrm{x})\omega^{\nu+2}+\Theta_2(\mathrm{x})\omega^{2\nu+2}\right]\\&-\frac{1}{2}\omega^{\nu}\left[\mathrm{x}^3\omega^2+\Theta_1(\mathrm{x})\omega^{\nu+2}+\Theta_2(\mathrm{x})\omega^{2\nu+2}\right].\end{aligned} \tag{32}$$

By dividing $\omega^{2\nu+2}$ on both sides of Eq. (32), we get

$$\begin{aligned}\frac{1}{\omega^{2\nu+2}}\mathrm{E}Res_2(\mathrm{x},\ \omega)=&\frac{1}{\omega^{\nu}}\Theta_1(\mathrm{x})+\Theta_2(\mathrm{x})+\frac{1}{\omega^{\nu+2}}\mathrm{x}^2\mathrm{D}_{\mathrm{xx}}\left[\mathrm{x}^3\omega^2+\Theta_1(\mathrm{x})\omega^{\nu+2}+\Theta_2(\mathrm{x})\omega^{2\nu+2}\right]\\&+\frac{1}{2}\frac{1}{\omega^{\nu+2}}\mathrm{x}\mathrm{D}_{\mathrm{x}}\left[\mathrm{x}^3\omega^2+\Theta_1(\mathrm{x})\omega^{\nu+2}+\Theta_2(\mathrm{x})\omega^{2\nu+2}\right]\\&-\frac{1}{\omega^{\nu+2}}\left[\mathrm{x}^3\omega^2+\Theta_1(\mathrm{x})\omega^{\nu+2}+\Theta_2(\mathrm{x})\omega^{2\nu+2}\right].\end{aligned} \tag{33}$$

Again use the fact that:

$$\lim_{\omega\to 0}\left(\frac{1}{\omega^{\Bbbk\nu+2}}\mathrm{E}Res_{\Bbbk}(\mathrm{x},\ \omega)\right)=0. \tag{34}$$

As a result, we obtained the $\Theta_2(\mathrm{x})$.

$$\Theta_2(\mathrm{x}) = (6.5)^2\mathrm{x}^3.$$

Consequently, the approximate solution derived from two iterations is provided below:

$$\aleph_2(\mathrm{x},\ \omega) = \omega^2\mathrm{x}^3 - 6.5\mathrm{x}^3\omega^{\nu+2} + (6.5)^2\mathrm{x}^3\omega^{2\nu+2}. \tag{35}$$

In particular, to determine the $\Theta_{\mathbb{k}}(\mathrm{x})$, first use the $\mathbb{k}$th-truncated series in Eq. (26), then utilize it in the $\mathbb{k}$th-ERF, dividing $\mathrm{E}Res_{\mathbb{k}}(\mathrm{x},\omega)$ by $\omega^{\mathbb{k}\nu+2}$, then solve the following formula:

$$\lim_{\omega\to 0}\left(\frac{1}{\omega^{\mathbb{k}\nu+2}}\mathrm{E}Res_{\mathbb{k}}(\mathrm{x},\ \omega)\right) = 0,\ \text{for}\ \Theta_{\mathbb{k}}(\mathrm{x}).$$

Through using the aforementioned process, we achieve the following outcomes:

$$\Theta_3(\mathrm{x}) = -(6.5)^3\mathrm{x}^3.$$

$$\Theta_4(\mathrm{x}) = (6.5)^4\mathrm{x}^3.$$

$$\Theta_5(\mathrm{x}) = -(6.5)^5\mathrm{x}^3.$$

After five iterations, the approximate solution to Eq. (23) is produced as:

$$\aleph_5(\mathrm{x},\ \omega) = \mathrm{x}^3\omega^2 - 6.5\mathrm{x}^3\omega^{\nu+2} + (6.5)^2\mathrm{x}^3\omega^{2\nu+2} - (6.5)^3\mathrm{x}^3\omega^{3\nu+2} + (6.5)^4\mathrm{x}^3\omega^{4\nu+2} - (6.5)^5\mathrm{x}^3\omega^{5\nu+2}. \tag{36}$$

By applying the E^{-1} to the Eq. (36) we are able to approximate the fifth step solution in the original feature space.

$$\Im_5(\mathrm{x},\ \tau) = \mathrm{x}^3 - \frac{6.5\mathrm{x}^3\tau^{\nu}}{\Gamma(\nu+1)} + \frac{(6.5)^2\mathrm{x}^3\tau^{2\nu}}{\Gamma(2\nu+1)} - \frac{(6.5)^3\mathrm{x}^3\tau^{3\nu}}{\Gamma(3\nu+1)} + \frac{(6.5)^4\mathrm{x}^3\tau^{4\nu}}{\Gamma(4\nu+1)} - \frac{(6.5)^5\mathrm{x}^3\tau^{5\nu}}{\Gamma(5\nu+1)}. \tag{37}$$

We have the following expression for $\nu = 1$:

$$\Im_5(\mathrm{x},\ \tau) = \mathrm{x}^3\left[1 + \frac{(-6.5\tau)}{1!} + \frac{(-6.5\tau)^2}{2!} + \frac{(-6.5\tau)^3}{3!} + \frac{(-6.5\tau)^4}{4!} + \frac{(-6.5\tau)^5}{5!}\right]. \tag{38}$$

Which are the first six terms of the expansion $\mathrm{x}^3e^{-6.5\tau}$, and thus is the exact solution of Eqs. (20) and (21) at $\nu = 1$.

Problem 4.2 The second model is as [29, 30]:

$$\frac{\partial^{\nu}\Im(\mathrm{x},\ \tau)}{\partial\tau^{\nu}}+0.08(2+\sin\mathrm{x})^{2}\mathrm{x}^{2}\frac{\partial^{2}\Im(\mathrm{x},\ \tau)}{\partial\mathrm{x}^{2}}+0.06\mathrm{x}\frac{\partial\Im(\mathrm{x},\ \tau)}{\partial\mathrm{x}}=0.06\Im(\mathrm{x},\ \tau),\ 0<\nu\leq 1, \tag{39}$$

with

$$\Im(\mathrm{x},\ 0)=\max(\mathrm{x}-25e^{-0.06},\ 0). \tag{40}$$

First, apply E to both sides of Eq. (39), and then use the initial condition from Eq. (40).

$$\begin{aligned}\aleph(\mathrm{x},\ \omega)=&\omega^{2}\max(\mathrm{x}-25e^{-0.06},\ 0)-\omega^{\nu}0.08(2+\sin\mathrm{x})^{2}\mathrm{x}^{2}\mathrm{D}_{\mathrm{xx}}\aleph(\mathrm{x},\ \omega)\\&-0.06\mathrm{x}\omega^{\nu}\mathrm{D}_{\mathrm{x}}\aleph(\mathrm{x},\ \omega)+0.06\omega^{\nu}\aleph(\mathrm{x},\ \omega).\end{aligned} \tag{41}$$

Suppose that the series solution of Eq. (41) is as follows:

$$\aleph(\mathrm{x},\ \omega)=\sum_{\mathrm{n}=0}^{\infty}\Theta_{\mathrm{n}}(\mathrm{x})\omega^{\mathrm{n}\nu+2}. \tag{42}$$

The $\Bbbk$th-truncated series of $\aleph(\mathrm{x},\ \omega)$ is given as:

$$\aleph_{\Bbbk}(\mathrm{x},\ \omega)=\sum_{\mathrm{n}=0}^{\Bbbk}\Theta_{\mathrm{n}}(\mathrm{x})\omega^{\mathrm{n}\nu+2}. \tag{43}$$

We obtained the following result by using the Lemma 1 (iii).

$$\Theta_{0}(\mathrm{x})=\lim_{\omega\to 0}\left(\frac{1}{\omega^{2}}\aleph(\mathrm{x},\ \omega)\right)=\Im(\mathrm{x},\ 0)=\max(\mathrm{x}-25e^{-0.06},\ 0). \tag{44}$$

So, the $\Bbbk$th-truncated series becomes as follows:

$$\aleph_{\Bbbk}(\mathrm{x},\ \omega)=\omega^{2}\max(\mathrm{x}-25e^{-0.06},\ 0)+\sum_{\mathrm{n}=1}^{\Bbbk}\Theta_{\mathrm{n}}(\mathrm{x})\omega^{\mathrm{n}\nu+2}. \tag{45}$$

The ERF of Eq. (41) is as follows:

$$\begin{aligned}\mathrm{E}Res(\mathrm{x},\ \omega)=&\aleph(\mathrm{x},\ \omega)-\omega^{2}\max(\mathrm{x}-25e^{-0.06},\ 0)+\omega^{\nu}0.08(2+\sin\mathrm{x})^{2}\mathrm{x}^{2}\mathrm{D}_{\mathrm{xx}}\aleph(\mathrm{x},\ \omega)\\&+0.06\mathrm{x}\omega^{\nu}\mathrm{D}_{\mathrm{x}}\aleph(\mathrm{x},\ \omega)-0.06\omega^{\nu}\aleph(\mathrm{x},\ \omega).\end{aligned} \tag{46}$$

The $\mathbb{k}$th-ERF of Eq. (41) is given below.

$$\mathrm{E}Res_{\mathbb{k}}(\mathrm{x},\ \omega) = \aleph_{\mathbb{k}}(\mathrm{x},\ \omega) - \omega^2 \max(\mathrm{x} - 25e^{-0.06},\ 0) + \omega^{\nu} 0.08(2+\sin \mathrm{x})^2 \mathrm{x}^2 \mathrm{D}_{\mathrm{xx}}\, \aleph_{\mathbb{k}}(\mathrm{x},\ \omega)$$

$$+ 0.06\mathrm{x}\omega^{\nu} \mathrm{D}_{\mathrm{x}}\, \aleph_{\mathbb{k}}(\mathrm{x},\ \omega) - 0.06\omega^{\nu}\, \aleph_{\mathbb{k}}(\mathrm{x},\ \omega). \tag{47}$$

To determine the first unknown coefficient $\Theta_1(\mathrm{x})$ in Eq. (43), we need to apply the $1st$-truncated expansion $\aleph_1(\mathrm{x},\ \omega) = \omega^2 \max(\mathrm{x} - 25e^{-0.06},\ 0) + \Theta_1(\mathrm{x})\omega^{\nu+2}$ into the $1st$-ERF $\mathrm{E}Res_1(\mathrm{x},\ \omega)$, divide by $\omega^{\nu+2}$ on both sides, and apply the following fact $\lim_{\omega\to 0}\left(\frac{1}{\omega^{\nu+2}}\mathrm{E}Res_1(\mathrm{x},\ \omega)\right) = 0$ to acquire

$$\Theta_1(\mathrm{x}) = -0.06[\mathrm{x} - \max(\mathrm{x} - 25e^{-0.06},\ 0)].$$

Similarly, to find the value of the second undefined coefficient $\Theta_2(\mathrm{x})$, we need to apply the $2nd$ truncated expansion $\aleph_2(\mathrm{x},\ \omega) = \omega^2 \max(\mathrm{x} - 25e^{-0.06},\ 0) + \Theta_1(\mathrm{x})\omega^{\nu+2} + \Theta_2(\mathrm{x})\omega^{2\nu+2}$ into the $2nd$-ERF and apply the following fact $\lim_{\omega\to 0}\left(\frac{1}{\omega^{2\nu+2}}\mathrm{E}Res_2(\mathrm{x},\ \omega)\right) = 0$, we have

$$\Theta_2(\mathrm{x}) = -(0.06)^2\big(\mathrm{x} - \max(\mathrm{x} - 25e^{-0.06},\ 0)\big).$$

The second iteration yielded the following approximate solution:

$$\aleph_2(\mathrm{x},\ \omega) = \omega^2\big(\max(\mathrm{x} - 25e^{-0.06},\ 0)\big) - 0.06\omega^{\nu+2}\big(\mathrm{x} - \max(\mathrm{x} - 25e^{-0.06},\ 0)\big)$$

$$- (0.06)^2\omega^{2\nu+2}\big(\mathrm{x} - \max(\mathrm{x} - 25e^{-0.06},\ 0)\big). \tag{48}$$

We carried out the identical procedure to ascertain the $3rd$, $4th$, and $5th$ unknown coefficients.

$$\Theta_3(\mathrm{x}) = -(0.06)^3\big(\mathrm{x} - \max(\mathrm{x} - 25e^{-0.06},\ 0)\big).$$

$$\Theta_4(\mathrm{x}) = -(0.06)^4\big(\mathrm{x} - \max(\mathrm{x} - 25e^{-0.06},\ 0)\big).$$

$$\Theta_5(\mathrm{x}) = -(0.06)^5\big(\mathrm{x} - \max(\mathrm{x} - 25e^{-0.06},\ 0)\big).$$

Thus, the approximate solution obtained from the $5th$ iteration of Eq. (41) is like this:

$$\aleph_5(\mathrm{x},\ \omega) = \omega^2\big(\max(\mathrm{x} - 25e^{-0.06},\ 0)\big) - \big[0.06\omega^{\nu+2} + (0.06)^2\omega^{2\nu+2} + (0.06)^3\omega^{3\nu+2} + (0.06)^4\omega^{4\nu+2}$$

$$+ (0.06)^5\omega^{5\nu+2}\big(\mathrm{x} - \max(\mathrm{x} - 25e^{-0.06},\ 0)\big). \tag{49}$$

The approximate solution obtained from the $5th$ iteration using ERM of Eqs. (39) and (40), using E^{-1} on both sides of Eq. (49), is as follows:

$$\Im_5(\mathrm{x},\ \tau) = \max(\mathrm{x} - 25e^{-0.06},\ 0) - \left[\frac{(0.06\tau^{\nu})}{\Gamma(\nu+1)} + \frac{(0.06\tau^{\nu})^2}{\Gamma(2\nu+1)} + \frac{(0.06\tau^{\nu})^3}{\Gamma(3\nu+1)} + \frac{(0.06\tau^{\nu})^4}{\Gamma(4\nu+1)}\right.$$

$$\left. + \frac{(0.06\tau^{\nu})^5}{\Gamma(5\nu+1)}\big(\mathrm{x} - \max(\mathrm{x} - 25e^{-0.06},\ 0)\big)\right]. \tag{50}$$

When $\nu = 1$ is used in Eq. (50), we get as follows:

$$\Im_5(\mathrm{x},\ \tau) = \max(\mathrm{x} - 25e^{-0.06},\ 0) - \left[0.06\tau + \frac{(0.06\tau)^2}{2!} + \frac{(0.06\tau)^3}{3!} + \frac{(0.06\tau)^4}{4!}\right.$$

$$\left. + \frac{(0.06\tau)^5}{5!}\big(\mathrm{x} - \max(\mathrm{x} - 25e^{-0.06},\ 0)\big)\right]. \tag{51}$$

Therefore, for $\nu = 1$, the exact solutions to Eqs. (39) and (40) are as follows:

$$\Im(\mathrm{x},\ \tau) = \max(\mathrm{x} - 25e^{-0.06},\ 0) + (1 - e^{0.06\tau})(\mathrm{x} - \max(\mathrm{x} - 25e^{-0.06},\ 0)).$$

Problem 4.3 The third model is given as in [29, 30]:

$$\frac{\partial^{\nu}\Im(\mathrm{x},\ \tau)}{\partial\tau^{\nu}} = \frac{\partial^2\Im(\mathrm{x},\ \tau)}{\partial\mathrm{x}^2} + (\Omega - 1)\frac{\partial\Im(\mathrm{x},\ \tau)}{\partial\mathrm{x}} - \Omega\Im(\mathrm{x},\ \tau),\ 0 < \nu \leq 1, \tag{52}$$

with

$$\Im(\mathrm{x},\ 0) = \max(e^{\mathrm{x}} - 1,\ 0). \tag{53}$$

The procedure outlined in Section 3 yields the following result:

$$\aleph(\mathrm{x},\ \omega) = \omega^2\max(e^{\mathrm{x}} - 1,\ 0) + \omega^{\nu}\mathrm{D}_{\mathrm{xx}}\aleph(\mathrm{x},\ \omega) + (\Omega - 1)\omega^{\nu}\mathrm{D}_{\mathrm{x}}\aleph(\mathrm{x},\ \omega) - \Omega\omega^{\nu}\aleph(\mathrm{x},\ \omega). \tag{54}$$

To explain the algebraic equation Eq. (54)'s expansion solution. Consequently, we presume that $\aleph(\mathrm{x},\ \omega)$ expands as follows:

$$\aleph(\mathrm{x},\ \omega) = \sum_{\mathrm{n}=0}^{\infty}\Theta_{\mathrm{n}}(\mathrm{x})\omega^{\mathrm{n}\nu+2}. \tag{55}$$

The following is the $\mathbb{k}$th-truncated expansion of Eq. (54):

$$\aleph_{\mathbb{k}}(\mathrm{x},\ \omega) = \omega^2 \max(e^{\mathrm{x}} - 1,\ 0) + \sum_{\mathrm{n}=1}^{\mathbb{k}} \Theta_{\mathrm{n}}(\mathrm{x})\omega^{\mathrm{n}\nu+2}. \tag{56}$$

The ERF of the Eq. (54) takes the following form

$$\mathrm{E}Res(\mathrm{x},\ \omega) = \aleph(\mathrm{x},\ \omega) - \omega^2 \max(e^{\mathrm{x}} - 1,\ 0) - \omega^{\nu}\mathrm{D}_{\mathrm{xx}}\aleph(\mathrm{x},\ \omega) - (\Omega - 1)\omega^{\nu}\mathrm{D}_{\mathrm{x}}\aleph(\mathrm{x},\ \omega) + \Omega\omega^{\nu}\aleph(\mathrm{x},\ \omega). \tag{57}$$

Accordingly, the $\mathbb{k}$th-ERF takes the form

$$\mathrm{E}Res_{\mathbb{k}}(\mathrm{x},\ \omega) = \aleph_{\mathbb{k}}(\mathrm{x},\ \omega) - \omega^2 \max(e^{\mathrm{x}} - 1,\ 0) - \omega^{\nu}\mathrm{D}_{\mathrm{xx}}\aleph_{\mathbb{k}}(\mathrm{x},\ \omega) - (\Omega - 1)\omega^{\nu}\mathrm{D}_{\mathrm{x}}\aleph_{\mathbb{k}}(\mathrm{x},\ \omega) + \Omega\omega^{\nu}\aleph_{\mathbb{k}}(\mathrm{x},\ \omega). \tag{58}$$

Transform the $\mathbb{k}$th-truncated series Eq. (56) into (57), multiply the result by $\omega^{\mathbb{k}\nu+2}$, and then solve the equation $\lim_{\omega\to 0}\left(\omega^{\mathbb{k}\nu+2}\mathrm{E}Res_{\mathbb{k}}(\mathrm{x},\ \omega)\right) = 0$, where $\mathbb{k} = 1,\ 2,\ 3,\ 4,\ 5$ for $\Theta_{\mathbb{k}}(\mathrm{x})$.

$$\Theta_0(\mathrm{x},\ \omega) = \max(e^{\mathrm{x}} - 1,\ 0).$$

$$\Theta_1(\mathrm{x},\ \omega) = \Omega[\max(e^{\mathrm{x}},\ 0) - \max(e^{\mathrm{x}} - 1,\ 0)].$$

$$\Theta_2(\mathrm{x},\ \omega) = -\Omega^2[\max(e^{\mathrm{x}},\ 0) - \max(e^{\mathrm{x}} - 1,\ 0)].$$

$$\Theta_3(\mathrm{x},\ \omega) = \Omega^3[\max(e^{\mathrm{x}},\ 0) - \max(e^{\mathrm{x}} - 1,\ 0)].$$

$$\Theta_4(\mathrm{x},\ \omega) = -\Omega^4[\max(e^{\mathrm{x}},\ 0) - \max(e^{\mathrm{x}} - 1,\ 0)].$$

$$\Theta_5(\mathrm{x},\ \omega) = \Omega^5[\max(e^{\mathrm{x}},\ 0) - \max(e^{\mathrm{x}} - 1,\ 0)].$$

Consequently, the following is the approximate solution obtained from the $5th$ iteration of Eq. (54):

$$\begin{aligned}\aleph_5(\mathrm{x},\ \omega) =& \omega^2 \max(e^{\mathrm{x}} - 1,\ 0) + \Omega\omega^{\nu+2}[\max(e^{\mathrm{x}},\ 0) - \max(e^{\mathrm{x}} - 1,\ 0)] \\ &- \Omega^2\omega^{2\nu+2}[\max(e^{\mathrm{x}},\ 0) - \max(e^{\mathrm{x}} - 1,\ 0)] + \Omega^3\omega^{3\nu+2}[\max(e^{\mathrm{x}},\ 0) - \max(e^{\mathrm{x}} - 1,\ 0)] \\ &- \Omega^4\omega^{4\nu+2}[\max(e^{\mathrm{x}},\ 0) - \max(e^{\mathrm{x}} - 1,\ 0)] + \Omega^5\omega^{5\nu+2}[\max(e^{\mathrm{x}},\ 0) - \max(e^{\mathrm{x}} - 1,\ 0)].\end{aligned} \tag{59}$$

The approximate solution obtained from the $5th$ iteration using ERM of Eqs. (52) and (53), using the E^{-1} on both sides of Eq. (59), is as follows:

$$\Im_5(\mathrm{x},\ \tau) = \max(e^{\mathrm{x}}-1,\ 0) + \frac{\Omega\tau^{\nu}}{\Gamma(\nu+1)}[\max(e^{\mathrm{x}},\ 0) - \max(e^{\mathrm{x}}-1,\ 0)] - \frac{\Omega^2\tau^{2\nu}}{\Gamma(2\nu+1)}$$

$$[\max(e^{\mathrm{x}},\ 0) - \max(e^{\mathrm{x}}-1,\ 0)] + \frac{\Omega^3\tau^{3\nu}}{\Gamma(3\nu+1)}[\max(e^{\mathrm{x}},\ 0) - \max(e^{\mathrm{x}}-1,\ 0)]$$

$$- \frac{\Omega^4\tau^{4\nu}}{\Gamma(4\nu+1)}[\max(e^{\mathrm{x}},\ 0) - \max(e^{\mathrm{x}}-1,\ 0)] + \frac{\Omega^5\tau^{5\nu}}{\Gamma(5\nu+1)}[\max(e^{\mathrm{x}},\ 0) - \max(e^{\mathrm{x}}-1,\ 0)]. \tag{60}$$

When $\nu = 1$ is used in Eq. (60), we get as follows:

$$\Im_5(\mathrm{x},\ \tau) = \max(e^{\mathrm{x}}-1,\ 0) + \left[\frac{\Omega\tau}{1!} - \frac{\Omega^2\tau^2}{2!} + \frac{\Omega^3\tau^3}{3!} - \frac{\Omega^4\tau^4}{4!} + \frac{\Omega^5\tau^5}{5!}\right][\max(e^{\mathrm{x}},\ 0) - \max(e^{\mathrm{x}}-1,\ 0)]. \tag{61}$$

Therefore, for $\nu = 1$, the exact solution to Eqs. (52) and (53) is given as follows:

$$\Im(\mathrm{x},\ \tau) = \max(e^{\mathrm{x}}-1,\ 0)e^{-\Omega\tau} + \max(e^{\mathrm{x}},\ 0)(1-e^{-\Omega\tau}).$$

5. Numerical simulation and discussion

In this section, the outcomes of the models addressed in Problems 4.1-4.3 are analyzed both graphically and numerically. Figures 1-3 illustrate two-dimensional plots comparing the exact solutions with the approximate solutions generated using the ERM. These figures present the graphical behavior of both solutions obtained through five iterations of ERM for different values of $\nu = 0.6,\ 0.7,\ 0.8,\ 0.9$, and 1.0, over the domain $\tau \in [0,\ 0.5]$. The plots clearly indicate that the approximate solutions progressively align with the exact ones as ν approaches 1.0. The intersection of the two solutions at $\nu = 1.0$ highlights the accuracy and reliability of the proposed method.

An error function serves as a useful tool for evaluating the precision of approximate analytical methods. Since the ERM yields an approximate analytical solution expressed through an infinite MFPS, reporting the associated errors is essential. To validate the accuracy of ERM, both recurrence and absolute error functions are utilized. Tables 1-3 present the numerical convergence of the approximate solutions obtained after five iterations, measured by the expression $|\ \Im^5(\varkappa,\ \tau) - \Im^4(\mathrm{x},\ \tau)\ |$ for various values of ν over the interval $\tau \in [0,\ 0.10]$. These tables reveal that the error term $|\ \Im^5(\mathrm{x},\ \tau) - \Im^4(\mathrm{x},\ \tau)\ |$ rapidly diminishes as ν approaches 1.0, thereby confirming the accuracy and convergence of the ERM.

Table 4-6 compares the absolute errors of the fifth-step approximations derived by ERM, PDTA [28], ADM [29], and Aboodh ADM [30] at feasible short-listed grid locations in the interval of $\tau \in [0,\ 10]$. The results acquired utilizing the recommended method show clear consensus with the PDTA, ADM, and Aboodh ADM, which confirms that the ERM is a good substitute to solve time-fractional BS models.

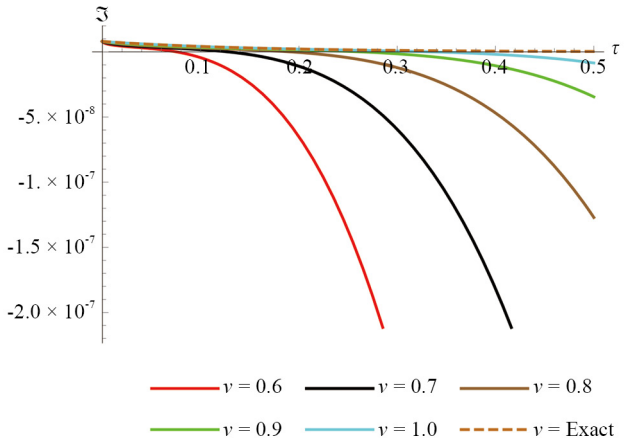

Figure 1. The 2-D plots of approximate and exact solutions to Problem 4.1 at various ν values when x = 0.002 in the $\tau \in [0,\ 0.5]$ interval

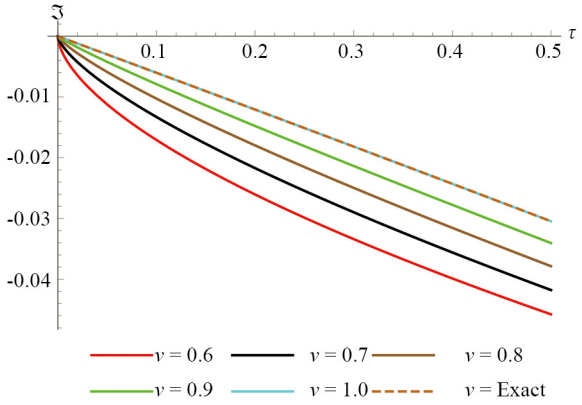

Figure 2. The 2-D plots of approximate and exact solutions to Problem 4.2 at various ν values when x = 1.0 in the $\tau \in [0,\ 0.5]$ interval

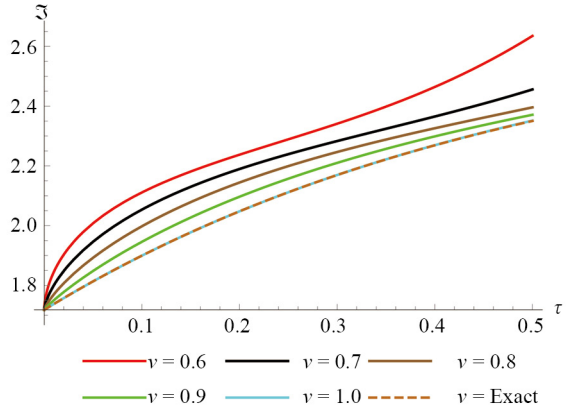

Figure 3. The 2-D plots of approximate and exact solutions to Problem 4.3 at different ν values when x = 1.0 and $\Omega = 2.0$ in the $\tau \in [0,\ 0.5]$ interval

Table 1. At different values of ν at x $= 0.002$, the $\mid \Im^5(x,\ \tau) - \Im^4(x,\ \tau) \mid$ of Problem 4.1 was found using ERM at reasonable points in the interval $\tau \in [0,\ 0.10]$

τ	$\nu = 0.7$	$\nu = 0.8$	$\nu = 0.9$	$\nu = 1.0$
0.01	8.11×10^{-13}	3.75×10^{-14}	1.80×10^{-15}	7.61×10^{-17}
0.02	8.97×10^{-12}	6.31×10^{-13}	4.12×10^{-14}	2.39×10^{-15}
0.03	3.81×10^{-11}	3.22×10^{-12}	2.56×10^{-13}	1.82×10^{-14}
0.04	1.04×10^{-10}	9.84×10^{-12}	8.99×10^{-13}	7.83×10^{-14}
0.05	2.28×10^{-10}	2.46×10^{-11}	2.39×10^{-12}	2.51×10^{-13}
0.06	4.29×10^{-10}	5.10×10^{-11}	5.71×10^{-12}	6.14×10^{-13}
0.07	7.31×10^{-10}	9.15×10^{-11}	1.14×10^{-11}	1.29×10^{-12}
0.08	1.15×10^{-9}	1.59×10^{-10}	2.08×10^{-11}	2.50×10^{-12}
0.09	1.74×10^{-9}	2.52×10^{-10}	3.47×10^{-11}	4.58×10^{-12}
0.10	2.53×10^{-9}	3.85×10^{-10}	5.59×10^{-11}	7.82×10^{-12}

Table 2. In Problem 4.2, the $\mid \Im^5(\alpha,\ \tau) - \Im^4(\alpha,\ \tau) \mid$ at different ν values at x $= 1.0$ was calculated using ERM at reasonable points in the interval $\tau \in [0,\ 0.10]$

τ	$\nu = 0.7$	$\nu = 0.8$	$\nu = 0.9$	$\nu = 1.0$
0.01	6.69×10^{-15}	3.24×10^{-16}	1.49×10^{-17}	6.48×10^{-19}
0.02	7.56×10^{-14}	5.18×10^{-15}	3.36×10^{-16}	2.07×10^{-17}
0.03	3.13×10^{-13}	2.62×10^{-14}	2.08×10^{-15}	1.57×10^{-16}
0.04	8.56×10^{-13}	8.29×10^{-14}	7.61×10^{-15}	6.64×10^{-16}
0.05	1.87×10^{-12}	2.03×10^{-13}	2.08×10^{-14}	2.03×10^{-15}
0.06	3.54×10^{-12}	4.20×10^{-13}	4.72×10^{-14}	5.04×10^{-15}
0.07	6.07×10^{-12}	7.78×10^{-13}	9.44×10^{-14}	1.09×10^{-14}
0.08	9.68×10^{-12}	1.33×10^{-12}	1.72×10^{-13}	2.12×10^{-14}
0.09	1.46×10^{-11}	2.13×10^{-12}	2.92×10^{-13}	3.83×10^{-14}
0.10	2.11×10^{-11}	3.24×10^{-12}	4.70×10^{-13}	6.48×10^{-14}

Table 3. At different values of ν at x $= 0.002$ when $\Omega = 2.0$, the $\mid \Im^5(x,\ \tau) - \Im^4(x,\ \tau) \mid$ of Problem 4.3 was calculated using ERM at reasonable locations in the region $\tau \in [0,\ 0.10]$

τ	$\nu = 0.7$	$\nu = 0.8$	$\nu = 0.9$	$\nu = 1.0$
0.01	2.75×10^{-7}	1.33×10^{-8}	6.11×10^{-10}	2.67×10^{-11}
0.02	3.11×10^{-6}	2.13×10^{-7}	1.38×10^{-8}	8.53×10^{-10}
0.03	1.29×10^{-5}	1.08×10^{-6}	8.58×10^{-8}	6.48×10^{-9}
0.04	3.52×10^{-5}	3.41×10^{-6}	3.13×10^{-7}	2.73×10^{-8}
0.05	7.69×10^{-5}	8.33×10^{-6}	8.54×10^{-7}	8.33×10^{-8}
0.06	1.46×10^{-4}	1.73×10^{-5}	1.94×10^{-6}	2.07×10^{-7}
0.07	2.50×10^{-4}	3.20×10^{-5}	3.88×10^{-6}	4.48×10^{-7}
0.08	3.98×10^{-4}	5.46×10^{-5}	7.08×10^{-6}	8.74×10^{-7}
0.09	6.02×10^{-4}	8.75×10^{-5}	1.20×10^{-5}	1.57×10^{-6}
0.10	8.70×10^{-4}	1.33×10^{-4}	1.93×10^{-5}	2.67×10^{-6}

Table 4. Absolute errors of ERM and PDTA for Problem 4.1 at x = 0.002 and $\tau = 1$ to 10

t	Exact solution $(0.002)^3 e^{-6.5\tau}$	Approximate solution $\Im_5(0.002,\ \tau)$	Absolute error ERM	Absolute error PDTA [28]
1	1.122×10^{-12}	2.273×10^{-12}	1.151×10^{-12}	1.151×10^{-12}
2	1.266×10^{-15}	3.559×10^{-15}	2.293×10^{-15}	2.293×10^{-15}
3	1.427×10^{-19}	5.574×10^{-19}	4.147×10^{-19}	4.147×10^{-19}
4	1.609×10^{-23}	8.729×10^{-23}	7.120×10^{-23}	7.120×10^{-23}
5	1.814×10^{-27}	1.367×10^{-26}	1.186×10^{-26}	1.186×10^{-26}
6	2.045×10^{-31}	2.141×10^{-30}	1.937×10^{-30}	1.937×10^{-30}
7	2.305×10^{-35}	3.353×10^{-34}	3.123×10^{-34}	3.123×10^{-34}
8	2.599×10^{-39}	5.251×10^{-38}	4.991×10^{-38}	4.991×10^{-38}
9	2.930×10^{-43}	8.223×10^{-42}	7.930×10^{-42}	7.930×10^{-42}
10	3.303×10^{-47}	1.288×10^{-45}	1.255×10^{-45}	1.255×10^{-45}

Table 5. Absolute errors of ERM, ADM, and Aboodh-ADM for Problem 4.2 at x = 1.0 and $\tau = 1$ to 10

τ	Exact solution $\Im(1.0,\ \tau)$	Approximate solution $\Im_5(1.0,\ \tau)$	Absolute error ERM	Absolute error ADM and Aboodh ADM [29, 30]
1	−0.061837	−0.061836	6.209×10^{-7}	6.209×10^{-7}
2	−0.127497	−0.127482	1.538×10^{-5}	1.538×10^{-5}
3	−0.197213	−0.197085	1.280×10^{-4}	1.280×10^{-4}
4	−0.271249	−0.270609	6.397×10^{-4}	6.397×10^{-4}
5	−0.349859	−0.347521	2.338×10^{-3}	2.338×10^{-3}
6	−0.433329	−0.426430	6.899×10^{-3}	6.899×10^{-3}
7	−0.521961	−0.504700	1.726×10^{-2}	1.726×10^{-2}
8	−0.616077	−0.578480	3.759×10^{-2}	3.759×10^{-2}
9	−0.716007	−0.642427	7.358×10^{-2}	7.358×10^{-2}
10	−0.822119	−0.690614	1.315×10^{-1}	1.315×10^{-1}

Table 6. Absolute errors of ERM, ADM, and Aboodh-ADM for Problem 4.3 at x = 1.0, $\Omega = 2.0$ and $\tau = 1$ to 10

τ	Exact solution $\Im(1.0,\ \tau)$	Approximate solution $\Im_5(1.0,\ \tau)$	Absolute error ERM	Absolute error ADM and Aboodh ADM [29, 30]
0.1	1.63746	1.63733	1.300×10^{-4}	1.300×10^{-4}
0.2	1.67032	1.66961	7.100×10^{-4}	7.100×10^{-4}
0.3	1.69768	1.69544	2.240×10^{-3}	2.240×10^{-3}
0.4	1.72006	1.71490	5.160×10^{-3}	5.160×10^{-3}
0.5	1.73794	1.72799	9.950×10^{-3}	9.950×10^{-3}
0.6	1.75173	1.73467	1.706×10^{-2}	1.706×10^{-2}
0.7	1.76179	1.73484	2.695×10^{-2}	2.695×10^{-2}
0.8	1.76844	1.72879	3.965×10^{-2}	3.965×10^{-2}
0.9	1.77196	1.71608	5.588×10^{-2}	5.588×10^{-2}
1.0	1.77259	1.69630	7.629×10^{-2}	7.629×10^{-2}

6. Conclusion

This research work presents, for the first time in the literature, a novel approach that combines the ET with residual functions to solve time-fractional BS models in the sense of the CD. Both approximate and exact solutions are obtained. Numerical and graphical results are provided to demonstrate the effectiveness of the proposed method. The recurrence errors obtained from the fifth-step approximate solutions for various values of ν are shown in Tables 1-3. The numerical results indicate that as $\nu \to 1.0$, the recurrence errors decrease, highlighting the efficiency of the approximation method. Tables 4-6 present a comparative study in terms of the absolute error obtained using ERM, PDTA, ADM, and the Aboodh ADM. The results from ERM are in excellent agreement with those obtained by PDTA, ADM, and the Aboodh ADM.

The following summarizes the main advantages of the ERM over alternative analytical approximation techniques: By relying solely on the concept of a zero-limit process, the ERM significantly reduces computational effort compared to the conventional residual series approach, which requires repetitive computation of fractional derivatives for each series coefficient. Moreover, the ERM does not require He's or Adomian polynomials, offering a clear advantage over hybrid methods that incorporate Adomian decomposition or homotopy perturbation. Consequently, methods such as the residual series approach and those based on He's or Adomian polynomials for solving FDEs can be effectively replaced by the ERM. Additionally, this method avoids the need to make strong assumptions about the system's physical parameters, addressing a common limitation of traditional perturbation-based techniques. Based on our findings, the ERM proves to be both accurate and easy to implement.

In the future, we will apply this approach to nonlinear systems of fractional equations.

Author contributions

"Conceptualization, M.I.L., D.B., M.A.Y., T.A., and P.O.M.; Funding acquisition, T.A. and P.O.M.; Investigation, M.I.L., D.B., M.A.Y., T.A., and P.O.M.; Methodology, M.I.L., D.B., M.A.Y., T.A., and P.O.M.; Project administration, D.B., T.A., and P.O.M.; Software, M.I.L. and M.A.Y.; Supervision, D.B. and P.O.M.; Writing- original draft, M.I.L. and M.A.Y.; Writing -review & editing, M.I.L. and M.A.Y. All authors have read and agreed to the published version of the manuscript."

Acknowledgements

The authors would like to thank Prince Sultan University for paying the APC and for the support through the TAS research lab.

Data availability statement

Data is contained within the article or supplementary material.

Conflict of interest

The authors declare no competing financial interest.

References

[1] Djaouti A, Liaqat M. Theoretical results on the pth moment of ϕ-Hilfer stochastic fractional differential equations with a pantograph term. *Fractal and Fractional*. 2025; 9(3): 134. Available from: https://doi.org/10.3390/fractalfract9030134.

[2] Yousif M, Agarwal R, Mohammed P, Lupas A, Jan R, Chorfi N. Advanced methods for conformable time-fractional differential equations: Logarithmic non-polynomial splines. *Axioms*. 2024; 13(8): 551. Available from: https://doi.org/10.3390/axioms13080551.

[3] Djaouti A, Khan Z, Liaqat M, Al-Quran A. Existence, uniqueness, and averaging principle of fractional neutral stochastic differential equations in the $\mathbb{L}^p$ space with the framework of the ψ-Caputo derivative. *Mathematics*. 2024; 12(7): 1037. Available from: https://doi.org/10.3390/math12071037.

[4] Lan K. Generalizations of Riemann-Liouville fractional integrals and applications. *Mathematical Methods in the Applied Sciences*. 2024; 47(16): 12833-12870. Available from: https://doi.org/10.1002/mma.10183.

[5] Rezapour S, Liaqat M, Etemad S. An effective new iterative method to solve conformable cauchy reactiondiffusion equation via the shehu transform. *Journal of Mathematics*. 2022; 2022(1): 4172218. Available from: https://doi.org/10.1155/2022/4172218.

[6] Caputo M, Cametti C. Diffusion through skin in the light of a fractional derivative approach: Progress and challenges. *Journal of Pharmacokinetics and Pharmacodynamics*. 2021; 48(1): 3-19. Available from: https://doi.org/10.1007/s10928-020-09715-y.

[7] Djaouti A, Liaqat M. Qualitative analysis for the solutions of fractional stochastic differential equations. *Axioms*. 2024; 13(7): 438. Available from: https://doi.org/10.3390/axioms13070438.

[8] Yousif M, Hamasalh F, Zeeshan A, Abdelwahed M. Efficient simulation of time-fractional Korteweg-de Vries equation via conformable-Caputo non-polynomial spline method. *PLOS ONE*. 2024; 19(6): e0303760. Available from: https://doi.org/10.1371/journal.pone.0303760.

[9] Vivas-Cortez M, Yousif M, Mahmood B, Mohammed P, Chorfi N, Lupas A. High-accuracy solutions to the time-fractional KdV-Burgers equation using rational non-polynomial splines. *Symmetry*. 2025; 17(1): 16. Available from: https://doi.org/10.3390/sym17010016.

[10] Liang Y, Wang K, Hou X. Multiple kink-soliton, breather wave, interaction wave and the travelling wave solutions to the fractional (2 + 1)-dimensional Boiti-Leon-Manna-Pempinelli equation. *Fractals*. 2025. Available from: https://doi.org/10.1142/S0218348X25500823.

[11] Khatun M, Arefin M, Akbar M, Uddin M. Existence and uniqueness solution analysis of time-fractional unstable nonlinear Schrodinger equation. *Results in Physics*. 2024; 57: 107363. Available from: https://doi.org/10.1016/j.rinp.2024.107363.

[12] Wang K. The generalized (3 + 1)-dimensional B-type Kadomtsev-Petviashvili equation: Resonant multiple soliton, N-soliton, soliton molecules and the interaction solutions. *Nonlinear Dynamics*. 2024; 112(9): 7309-7324. Available from: https://doi.org/10.1007/s11071-024-09356-7.

[13] Wang K. The perturbed Chen-Lee-Liu equation: Diverse optical soliton solutions and other wave solutions. *Advances in Mathematical Physics*. 2024; 2024(1): 4990396. Available from: https://doi.org/10.1155/2024/4990396.

[14] Wang K, Wang G. He's variational method for the time-space fractional nonlinear Drinfeld-Sokolov-Wilson system. *Mathematical Methods in the Applied Sciences*. 2023; 46(7): 7798-7806. Available from: https://doi.org/10.1002/mma.7200.

[15] Wang K, Zhu H, Li S, Shi F, Li G, Liu X. Bifurcation analysis, chaotic behaviors, variational principle, Hamiltonian and diverse optical solitons of the fractional complex Ginzburg-Landau model. *International Journal of Theoretical Physics*. 2025; 64(5): 134. Available from: https://doi.org/10.1007/s10773-025-05977-9.

[16] Abd-Elhameed W, Youssri Y. Fifth-kind orthonormal Chebyshev polynomial solutions for fractional differential equations. *Computational and Applied Mathematics*. 2018; 37(3): 2897-2921. Available from: https://doi.org/10.1007/s40314-017-0488-z.

[17] Liaqat M, Khan A, Alam M, Pandit M. A highly accurate technique to obtain exact solutions to time-fractional quantum mechanics problems with zero and nonzero trapping potential. *Journal of Mathematics*. 2022; 2022(1): 9999070. Available from: https://doi.org/10.1155/2022/9999070.

[18] Hedayati M, Ezzati R. A new operational matrix method to solve nonlinear fractional differential equations. *Nonlinear Engineering*. 2024; 13(1): 20220364. Available from: https://doi.org/10.1515/nleng-2022-0364.

[19] Liaqat M, Khan A, Alqudah M, Abdeljawad T. Adapted homotopy perturbation method with Shehu transform for solving conformable fractional nonlinear partial differential equations. *Fractals*. 2023; 31(2): 2340027. Available from: https://doi.org/10.1142/S0218348X23400273.

[20] Wang K. A fast insight into the optical solitons of the generalized third-order nonlinear Schrödinger's equation. *Results in Physics*. 2022; 40: 105872. Available from: https://doi.org/10.1016/j.rinp.2022.105872.

[21] Wang K. Resonant multiple wave, periodic wave and interaction solutions of the new extended (3 + 1)-dimensional Boiti-Leon-Manna-Pempinelli equation. *Nonlinear Dynamics*. 2023; 111(17): 16427-16439. Available from: https://doi.org/10.1007/s11071-023-08699-x.

[22] Wang K, Shi F, Liu J. Soliton molecules and the novel hybrid interaction solutions of the new extended (3 + 1)-dimensional Boiti-Leon-Manna-Pempinelli equation. *Pramana*. 2024; 98(2): 67. Available from: https://doi.org/10.1007/s12043-024-02747-w.

[23] Djaouti A, Khan Z, Liaqat M, Al-Quran A. A novel technique for solving the nonlinear fractional-order smoking model. *Fractal and Fractional*. 2024; 8(5): 286. Available from: https://doi.org/10.3390/fractalfract8050286.

[24] Khan A, Liaqat M, Mushtaq A. Analytical analysis for space fractional helmholtz equations by using the hybrid efficient approach. *Acta Mechanica and Automatica*. 2024; 18(4): 116-125. Available from: https://doi.org/10.2478/ama-2024-0065.

[25] Liaqat M, Akgül A. Approximate and exact solutions of some nonlinear differential equations using the novel coupling approach in the sense of conformable fractional derivative. *Contemporary Mathematics*. 2024; 4132-4160. Available from: https://doi.org/10.37256/cm.5420245244.

[26] Nuugulu S, Patidar K, Tarla D. A physics informed neural network approach for solving time fractional Black-Scholes partial differential equations. *Optimization and Engineering*. 2024; 1-30. Available from: https://doi.org/10.1007/s11081-024-09910-7.

[27] Kadalbajoo M, Tripathi L, Kumar A. A cubic B-spline collocation method for a numerical solution of the generalized Black-Scholes equation. *Mathematical and Computer Modelling*. 2012; 55: 1483-1505. Available from: https://doi.org/10.1016/j.mcm.2011.10.040.

[28] Edeki S, Ugbebor O, Owoloko E. Analytical solution of the time-fractional order Black-Scholes model for stock option valuation on no dividend yield basis. *IAENG International Journal of Applied Mathematics*. 2017; 47: 407-416.

[29] Yavuz M, Ozdemir N. A different approach to the European option pricing model with new fractional operator. *Mathematical Modelling of Natural Phenomena*. 2018; 13: 12. Available from: https://doi.org/10.1051/mmnp/2018009.

[30] Alfaqeih S, Ozis T. Solving fractional Black-Scholes European option pricing equations by Aboodh transform decomposition method. *Palestinian Journal of Mathematics*. 2020; 9(2): 915-924.

[31] Saratha S, Krishnan G, Bagyalakshmi M, Lim C. Solving Black-Scholes equations using fractional generalized homotopy analysis method. *Computational and Applied Mathematics*. 2020; 39: 1-35. Available from: https://doi.org/10.1007/s40314-020-01306-4.

[32] Edeki S, Jena R, Chakraverty S, Baleanu D. Coupled transform method for time-space fractional Black-Scholes option pricing model. *Alexandria Engineering Journal*. 2020; 59(5): 3239-3246. Available from: https://doi.org/10.1016/j.aej.2020.08.031.

[33] Ankudinova J, Ehrhardt M. On the numerical solution of nonlinear Black-Scholes equations. *Computers and Mathematics with Applications*. 2008; 56(3): 799-812. Available from: https://doi.org/10.1016/j.camwa.2008.02.005.

[34] Golbabai A, Nikan O, Nikazad T. Numerical analysis of time fractional Black-Scholes European option pricing model arising in financial market. *Computational and Applied Mathematics*. 2019; 38: 1-24. Available from: https://doi.org/10.1007/s40314-019-0957-7.

[35] Kumar S, Yildirim A, Khan Y, Jafari H, Sayevand K, Wei L. Analytical solution of fractional Black-Scholes European option pricing equation by using Laplace transform. *Journal of Fractional Calculus and Applications*. 2012; 2(8): 1-9.

[36] Nikan O, Rashidinia J, Jafari H. An improved local radial basis function method for pricing options under the time-fractional Black-Scholes model. *Journal of Computational Science*. 2025; 89: 102610. Available from: https://doi.org/10.1016/j.jocs.2025.102610.

[37] Nikan O, Rashidinia J, Jafari H. Numerically pricing American and European options using a time fractional Black-Scholes model in financial decision-making. *Alexandria Engineering Journal*. 2025; 112: 235-245. Available from: https://doi.org/10.1016/j.aej.2024.10.083.

[38] Elzaki T, Abd Elmohmoud E. A novel approach to solving fractional Navier-Stokes equations using the Elzaki transform. *Fractal and Fractional*. 2025; 9(6): 396. Available from: https://doi.org/10.3390/fractalfract9060396.

[39] Liaqat M, Khan A, Akgul A, Ali M. A novel numerical technique for fractional ordinary differential equations with proportional delay. *Journal of Function Spaces*. 2022; 2022(1): 6333084. Available from: https://doi.org/10.1155/2022/6333084.